Characterization of Cellulose Nanocrystal Surfaces by SPM

R.R, Lahiji[1,2], R. Reifenberger[1,2], A. Raman[1,3], Alan Rudie[4], and R. J. Moon[1,4,5]

[1]Birck Nanotechnology Center, Purdue University
[2]Department of Physics, Purdue University
[3]School of Mechanical Engineering, Purdue University
[4]US Forest Service, Forest Products Laboratory
[5]School of Materials Engineering, Purdue University

ABSTRACT

Scanning probe microscopy (SPM) techniques have been used to investigate cellulose nanocrystal (CNC) surface chemistry and mechanical properties. Atomic force microscopy (AFM) was used to measure topography, stiffness, and pull-off force of CNC surfaces exposed to N_2 atmosphere with a 0.1% relative humidity (RH). Changes in the stiffness and pull-off force as a function of location along CNC surfaces were used to assess the uniformity in mechanical properties and surface chemistry, respectively. This work showed that the contact geometry affected all measurements and needs to be accounted for in the data analysis. Qualitatively, after taking into consideration effects of contact geometry, we find that the stiffness and pull-off force were reasonably uniform across the CNC length.

Keywords: atomic force microscopy, cellulose nanocrystals, relative humidity, topography, stiffness, pull-off force

1 INTRODUCTION

Cellulose is the world's most abundant biopolymer and is present in virtually all plants. Its main function is to act as a reinforcement material. Cellulose is a linear chain of ringed glucose molecules ($(C_6H_{10}O_5)_n$; n=10,000 to 15,000) linked together through an oxygen covalently bonded to C1 of one glucose ring and C4 of the adjoining ring[1, 2] (Figure 1a). Multiple cellulose chains hydrogen bond to each other forming cellulose fibrils (length: tens of microns, diameter: 2-20nm) having regions that are disordered (amorphous-like) or highly ordered (crystalline). The amorphous regions of the cellulose fibrils can be selectively hydrolyzed by acid, leaving behind the less reactive crystalline regions as nanometer-sized rods or whiskers (length: 100 to 300 nm, diameter: 3 to 5 nm) commonly referred to as Cellulose Nanocrystals (CNC)[3]. The tensile modulus along the length of these CNCs has been measured at 145 GPa,[4] which is greater than that of Kevlar® (130 GPa). Figure 1b schematically shows the orientation of the crystalline cellulose chains within a CNC.

CNCs offer several advantages as a reinforcement particle in polymer matrix composites. They have a high aspect ratio, a high stiffness, a low density (1.59 g/cm^3)[1], and have mechanical properties that are in the range for typical reinforcement materials (Table 1). Furthermore, they are made from sustainable resources that are biodegradable, potentially offering low environmental and animal health risks. They offer lower production costs relative to metal, ceramic or carbon based nanomaterials.[2] Their reactive surface readily facilitates grafting chemical species to achieve different surface properties (surface functionalization).[2, 5] The ability to chemically modify surface properties expands potential applications by enabling CNC dispersal in a wide range of matrix materials.

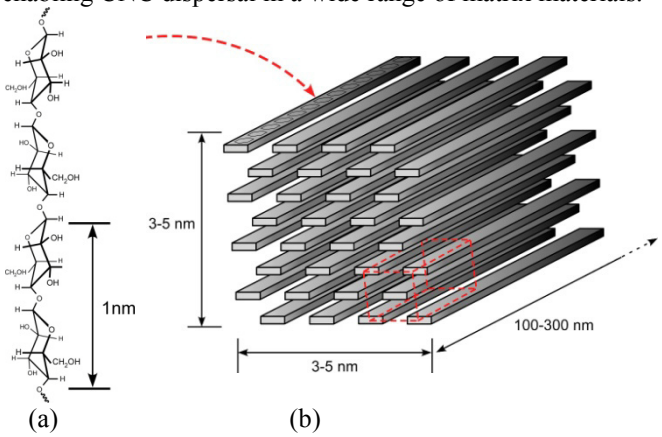

Figure 1: A schematic diagram of (a) segment of a cellulose chain, (b) the monoclinic arrangement of cellulose chains in a cellulose nanocrystal.

Material	Tensile strength (GPa)	Modulus (GPa)
CNCs	7.5	145
Glass fiber	4.8	86
Steel wire	4.1	207
Kevlar	3.8	130
Graphite whisker	21	410
Carbon nanotubes	11–73	270–970

Table 1: Properties of reinforcement materials[6]

The addition of CNCs to bulk composites, panels, or thin films has been demonstrated to modify thermal stability[7], mechanical strength[5], stiffness[8], toughness, and flexibility.[9] The arrangement of CNCs within

composites and films has a major effect on the final properties. Chemical treatments to tailor the CNC surface chemistry are being explored for controlling the degree of dispersion within the polymer matrices and to improve the strength of the resulting composite structure.[7] Some potential consumer applications for CNCs will be in the production of biodegradable, lightweight, and high-strength composite panels in the electronics, automotive, and aerospace industries.

AFM has been used extensively for imaging cellulose[2], typically to quantify the CNC aspect ratio resulting from a particular production process[3] or cellulose source (plant, wood, algae, or bacteria). Near-atomic resolution AFM topography imaging has confirmed the cellulose surface crystalline structure[10], in which different features on the CNC surface were assigned to the repeating functional groups of the cellulose crystalline structure (i.e. glucose rings, hydroxyl groups, etc). However, there have been no studies using AFM to describe the uniformity of CNC surface chemistry or measure mechanical properties perpendicular to the cellulose length axis.

2 EXPERIMENTAL PROCEDURE

2.1 CNC Processing

The CNCs preparation procedure follows those developed by Rånby[11]and modified by Beck-Candanedo et al.[3]. Acid hydrolysis was completed using a 8 to 1 weight ratio of 64% sulfuric acid to commercial grade dissolving pulp at 45° C for 1 hour. This mixture was then diluted with deionized water to quench the reaction, centrifuged, washed, underwent dialysis for about a week to remove any remaining acid, and ultrasonicated to provide mechanical agitation to further disperse the cellulose crystals. A final centrifuge separation step is used to remove the larger agglomerates in the CNC suspension.

2.2 AFM Measurement

AFM imaging was performed on CNCs deposited on mica substrates. A few drops of CNC solution (~2wt% suspension) was deposited onto a 1 cm by 1 cm square of freshly cleaved mica. The sample was rinsed with de-ionized water and blown dry with N_2 gas. This method resulted in well dispersed CNCs on the mica substrate.

AFM studies using a Nanotec Electronica scanning probe instrument were conducted in a humidity chamber set to either ambient conditions or to ~0.1% RH by flowing N_2 gas from liquid nitrogen boil-off into the chamber. WSxM software[12] (version 11.3) was used to process the AFM images. Mikromasch ultrasharp CSC37/NoAl cantilevers having a nominal tip radius of 10nm, nominal spring constant of 0.65 N/m and a nominal resonant frequency of 41 KHz were used in this study. For each cantilever, the spring constant was calibrated using Sader's method[13]. The spring constant of the cantilever used to obtain the data presented in Figures 3 was 2.22 N/m.

Imaging was performed using two different modes. Most topography imaging was completed using Dynamic mode AFM with an amplitude set point of 90% of A_o where A_o is the free cantilever amplitude of ~80 nm. Jumping mode AFM[14] was also used to acquire force vs. distance (F(z)) data using WSxM's general spectroscopy imaging (GSI) software. From the acquired F(z) data at every imaging point, stiffness and pull-off force as function of position across an image could be inferred. The maximum resolution in the GSI mode is 128×128 points over a specified scan area. Therefore, when scanning an area of say 800 nm × 800 nm, the separation between each data point is ~6.25nm

Stiffness was estimated from the slope of the F(z) data after AFM tip contact had been established, while the pull-off force was estimated from the discontinuity in F(z) data during AFM tip withdrawal. The protocols for such an analysis are well established and are described elsewhere in detail[15]. The stiffness and pull-off force measurements from the F(z) data were used to assess the uniformity of the CNC elastic response and surface chemistry.

3 EXPERIMENTAL RESULTS

3.1 AFM Imaging of CNCs

Topographic images from 20 different samples showed that the CNCs were on average ~150-300 nm in length, and 4-10nm in diameter; consistent with other studies.[3] The diameter of each CNC is typically found to vary along its length, suggesting that the removal of cellulose from the CNC surface is variable. Figure 2 shows a typical AFM topography image of CNCs on a mica surface as imaged under ambient conditions. AFM images reveal a significant distortion in the lateral size of a CNC due to well-known tip dilation effects. The CNC diameters were determined from the measured heights within the topography maps.

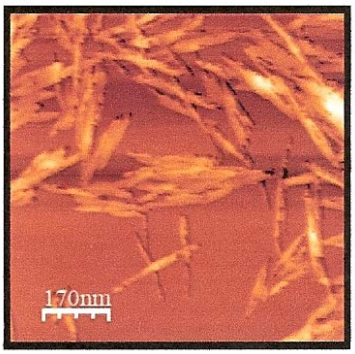

Figure 2: A dynamic mode AFM topographic image of a typical CNC sample.

3.2 Force verse Distance Results

We have used F(z) data obtained from the GSI mode to extract the stiffness and pull off forces from a CNC surface as compared to the mica substrate. Here we summarize our results on two different CNCs. The stiffness and pull off force obtained from the F(z) data for a single CNC (designated CNC-1) are plotted in Figure 3, while Table 2 summarizes average data from both CNC-1 and CNC-2 (and the nearby substrate regions designated Mica-1 and Mica-2).

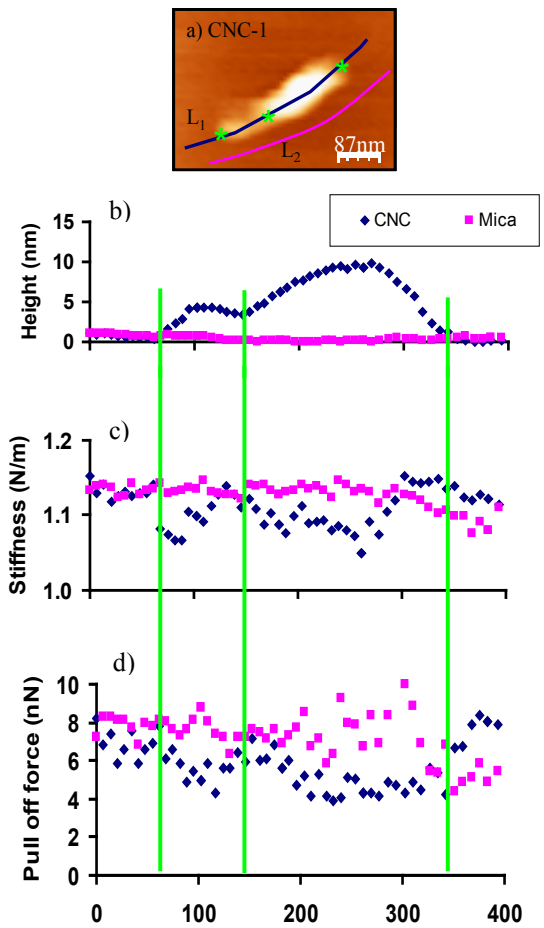

Figure 3. Summary of GSI results for CNC-1 in flowing N_2 gas (0.1% RH) conditions. (a) AFM topography, L_1 and L_2 are line profiles along CNC-1 and the mica substrate, respectively. (b) height profile along L_1 and L_2. (c) stiffness profile along L_1 and L_2. (d) AFM tip pull-off force profile along L_1 and L_2. The vertical green lines indicate the location of the CNC edges and the middle line marks the transition from small to large CNC diameter.

Figure 3a is a topography image (acquired in GSI mode) of CNC-1 and shows the location of line profiles used for the subsequent data plots. In Figure 3a, the line L_1 is drawn to transverse the mica surface for ~75 nm, then transverse the entire CNC length along the mid-point for ~275nm, and finally transverse the mica for ~50 nm. The line L_2 transverses the mica surface (Mica-1) next to CNC-1. The height profiles (Figure 3b) show a flat mica surface, while the CNC-1 height varies from 4 nm to 10 nm.

The stiffness profiles in Figure 3c allow a relative comparison between CNC-1 and mica. The stiffness of mica is essentially constant, exhibiting a ~5% decrease at the end of line L_2. For CNC-1, the stiffness profile is more variable and appears to be lower than for mica. The average stiffness of Mica-1 was 1.13±0.01 N/m while the average stiffness of CNC-1 was 1.10±0.02 N/m. The small scatter in the stiffness measurement suggests that trends are real. Additionally, for the L_1 profile, the stiffness values on mica match that from the L_2 profile, showing consistency in the measurement.

Figure 3d compares the pull-off force on CNC-1 to that of Mica-1. The pull-off force of mica was variable as exhibited by the data scatter. In contrast, the CNC pull-off force scatter was less, suggesting that the apparent changes in pull-off force as a function location may be real, and that the average pull-off force from CNC-1 was less than mica. The average pull off force on CNC-1 was 5.1±0.8 nN, and Mica-1 is 7.6±1.0 nN.

Similar trends were observed for CNC-2 and Mica-2, except that the CNC-2 height was more uniform at ~4nm. The average stiffness and pull-off values were comparable to CNC-1 and Mica-1 (see Table 2). Comparisons between CNC and mica show that under low relative humidity conditions, the measured stiffnesses are similar, but the pull off force from a CNC is lower than from mica.

Material	Height (nm)	Stiffness (N/m)	Pull-off Force (nN)
CNC-1	4-10	1.10 ± 0.02	5.1 ± 0.8
CNC-2	2-5	1.13 ± 0.01	5.1 ± 0.6
Mica-1	0-1	1.13 ± 0.01	7.6 ± 1.0
Mica-2	0-1	1.14 ± 0.01	8.1 ± 1.1

Table 2: Average height, stiffness and pull-off force for two different CNCs.

4 DISCUSSION

This preliminary study exploited SPM methods to qualitatively evaluate the uniformity of cellulose nanocrystal (CNC) surface chemistry and mechanical properties. A more quantitative analysis must better account for numerous geometrical effects (AFM tip dilation, edge effects, changing CNC height, AFM tip blunting, and radius of curvature of contacting surface) between the AFM tip and the appropriate contact surface.

Non-uniformities in the stiffness and pull-off force measurements are expected when the AFM tip contact with the CNC is off the center axis. To reduce these edge effects, line profiles were intentionally selected from the mid-point along the CNC length, thus increasing the consistency of the contact geometry for each measurement point.

Any change in CNC height (Figure 3b) provides a similar non-uniform contact issue as edge effects. As a result, variable stiffness and pull-off forces are expected due to changes in topography along the CNC. Evidence supporting this view are evident in Figure 3, in which the stiffness and pull-off force appear to change not only near the two ends of the CNC (at ~75nm and 350nm), but also near the topography maximum/minimum points (~100nm, 145nm, 250nm). By taking this into consideration, the stiffness and pull-off force measured along a CNC might be more uniform than suggested in Figure 3.

The different radius of curvature for the CNC as compared to the "flat" mica surface will alter the contact tip contact area and may skew any direct comparisons between CNCs and mica. For the results given in Figure 3 and Table 2, it may be inappropriate at this stage to attribute differences in the average stiffness and pull-off force between CNC and mica with differences in mechanical properties or surface chemistry. Such conclusions can only be firmly drawn after addressing questions related to possible different tip contact areas between a CNC and mica.

Taking into consideration possible artifacts resulting from the effects of contact geometry, several conclusions can be made from the work described above: (i) individual CNCs have a variable diameter; (ii) good consistency was observed in measurements of the average stiffness and pull-off force between two different CNCs, as well as for the two mica surfaces; and (iii) stiffness and pull-off force were found to be relatively uniform along the length of a CNC.

Future work will further develop advanced testing protocols to better account for artifacts inherent in the measurements, including contact geometry effects and water meniscus formation at the contact point between the AFM tip and surface. Numerical simulations will provide a more quantitative interpretation of the contact geometry effects of the contacting surface radius of curvature, the changing CNC height, and AFM tip blunting. Imagining the AFM tip (by SEM) before and after F(z) testing will quantify changes in tip shape. Additional testing in variable relative humidity and immersion under different liquids and gases will be used to study the influence of testing environment on the measurements.

REFERENCES

[1] A. C. O'Sullivan, "Cellulose: the structure slowly unravels," *Cellulose*, vol. 4, pp. 173-207, 1997.

[2] M. A. S. A. Samir, F. Alloin, and A. Dufresne, "Review of Recent Research into Cellulosic Whiskers, Their Properties and Their Application in Nanocomposite Field," *Biomacromolecules,* vol. 6, pp. 612-626, 2005.

[3] S. Beck-Candanedo, M. Roman, and D. G. Gray, "Effect of Reaction Conditions on the Properties and Behavior of Wood Cellulose Nanocrystal Suspensions," *Biomacromolecules*, vol. 6, pp. 1048-1054, 2005.

[4] A. Sturcova, G. R. Davies, and S. J. Eichhorn, "The elastic modulus and stress-transfer properties of tunicate cellulose whiskers," *Biomacromolecules*, vol. 6, pp. 1055-1061, 2005.

[5] W. J. Orts, J. Shey, S. H. Imam, G. M. Glenn, M. E. Buttman, and J.-F. Revol, "Application of Cellulose Microfibrils in Polymer Nanocomposites," *J. Polymer and the Environment*, vol. 13, pp. 301-306, 2005.

[6] http://woodscience.oregonstate.edu/faculty/simonsen.

[7] L. Petersson, I. Kvien, and K. Oksman, "Structure and thermal properties of poly(lactic acid)/cellulose whiskers nanocomposite materials," *Comp. Sci & Techn*, vol. 67, pp. 2535-2544, 2007.

[8] S. Noorani, J. Simonsen, and S. Atre, "Nano-enabled microtechnology: polysulfone nanocomposites incorporation cellulose nanocrystals," *Cellulose*, vol. 14, pp. 577-584, 2007.

[9] F. Dalmas, L. Chazeau, C. Cauthier, J.-Y. Cavaille, and R. Dendievel, "Large deformation mechanical behavior of flexible nanofiber filled polymer nanocomposites," *Polymer*, vol. 2006, pp. 2802-2812.

[10] A. A. Baker, W. Helbert, J. Sugiyama, and M. J. Miles, "New Insight into cellulose structure by atomic force microscopy shows the Ia crystal phase at near-atomic resolution," *Biophysical J.*, vol. 79, pp. 1139-1145, 2000.

[11] Ranby and G. Bengt, "The Cellulose Micelles," *Tappi J.*, vol. 35, pp. 53-58, 1952.

[12] I. Horcas, R. Fernandez, J. M. Gomez-Rodriguez, J. Colchero, J. Gomez-Herrero, and A. M. Baro, "WSXM: A software for scanning probe microscopy and a tool for nanotechnology," *Review of Scientific Instruments*, vol. 78, Jan. 2007.

[13] J. E. Sader, I. Larson, P. Mulvaney, and L. R. White, "Method for the calibration of atomic force microscope cantilevers," *Review of Scientific Instruments*, vol. 66, pp. 3789-3798, 1995.

[14] P. J. de Pablo, J. Gomez-Herrero, and A. M. Baro, "Jumping mode scanning force microscopy," *Appl. Phys. Lett.*, vol. 73, p. 3300, 1998.

[15] P. J. de Pablo, J. Colchero, J. Gomez-Herrero, A. M. Baro, D. M. Schaefer, S. Howell, B. Walsh, and R. Reifenberger, "Adhesion maps using scanning froce microscopy techniques," *Journal of Adhesion*, vol. 71, pp. 339-356, 1999.

ACKNOWLEDGMENTS

The authors thank Rick Riener for processing of the cellulose nanocrystals used in this study. This work was partially supported by the United States Forest Service.

In: NSTI Nanotechnology Conference and Trade Show Nanotechnology 2008 Vol. 103 CDROM. 2008 June 1-5; Bosdton, Massachusetts. Boca Raton, FL: CRC Press. 2: 704-707. ISBN: 978-1-4200-8511-2.